RAL-85-062

Science and Engineering Research Council
Rutherford Appleton Laboratory
CHILTON, DIDCOT, OXON

Two Phase Transitions in Nematic Droplets

R D Williams

July 1985

RAL-85-062

RAL 85 062

TWO PHASE TRANSITIONS IN NEMATIC DROPLETS

R D Williams
Rutherford Appleton Laboratory
Chilton, Didcot, Oxon, OX11 0QX, UK

Abstract

In an axisymmetric approximation we demonstrate a parity-breaking phase transition to a twisted configuration in tangentially anchored nematic liquid crystal droplets. The twisted phase occurs when $K_{11} > K_{22} + 0.431\ K_{33}$. In a magnetic field there is another phase transition corresponding to the droplet axis changing from parallel to normal to the field.

1. Introduction

A nematic liquid crystal is anisotropic, for the rod-like molecules are on average parallel to a unit vector $\underline{n}$. On macroscopic scales, $\underline{n}$ is a continuous field $\underline{n}(\underline{x})$, and an elastic energy density is associated with the squares of gradients of $\underline{n}$. Thus the elastic energy of a volume of nematic is proportional to the linear dimension L of the volume. For a compact volume, such as a drop of nematic suspended in isotropic fluid, there is also surface energy, proportional to L^2. Thus the internal energy of a large drop is dominated by the surface energy, and so the drop is spherical. At the nematic surface, there is energy per unit area associated with deviations of the anchoring angle from the easy angle[1]. By the same dimensional reasoning as above (given more explicitly in Section 2) the anchoring angle is always the easy angle: so-called strong anchoring.

If the director at the surface is normal to the surface, the director points radially from the centre of the sphere, with perhaps a twist. If the easy angle is between 0 and 90° (conical boundary conditions), then the position of the singularities in $\underline{n}$ change continuously with the elastic constants and also with the easy angle[3]. Furthermore there are problems from the sign ambiguity of $\underline{n}$, which arise for the following reason. Although the ends of a nematogen molecule are in general different, the energy difference between a parallel and an antiparallel pair is much smaller than the temperature, so ordering in direction $\underline{n}$ is physically the same as ordering in direction $-\underline{n}$. Thus there may be "branch-cut surfaces" across which $\underline{n}$ changes sign. If one of these surfaces is bounded in part by the surface of the sphere and in part by a line disclination, then it cannot be removed, only moved. This is analogous to the representation of an angle by a real number: the number can have discontinuities of 2π even though the underlying angle is continuous.

The situation is considerably simpler when the director is tangential to the surface. The bipolar configuration, suggested by Chandrasekhar[4] and experimentally verified by Dubois-Violette and Parodi[5], seems to be adopted by many nematics. The director is parallel to curves which join two diametrically opposite points of the surface of the drop, these curves lying on planes of constant azimuth. Twisted bipolar configurations (cf

Figure 2) have been observed[3]; with the limiting case of these twisted drops where the director is in the azimuthal direction like the magnetic field of a straight wire: we call this the toroidal configuration.

In this paper we examine tangentially anchored nematic drops, using the topology of the untwisted bipolar configuration, but with varying amounts of twist in the director field. We find that when the splay constant is small, the droplet is untwisted and when the splay constant is large, the droplet is twisted. This breaking of parity symmetry is associated with a second-order phase transition.

Since nematogen molecules tend to be parallel to a magnetic field, we expect the axis of an untwisted drop (when the splay constant is small) to be parallel to the field, and that of a very twisted toroidal drop perpendicular. There is a second order transition between these phases, associated with a breaking of axial symmetry.

Theory

If a droplet of nematic is sufficiently large and in an isotropic environment, it will be spherical. The droplet is characterised by a unit-vector director $\underline{n}(\underline{x})$, and the Frank elastic energy per unit volume[6] is

$$F = \tfrac{1}{2}K_{11}(\mathrm{div}\underline{n})^2 + \tfrac{1}{2}K_{22}(\underline{n}.\mathrm{curl}\underline{n})^2 + \tfrac{1}{2}K_{33}(\underline{n}\times\mathrm{curl}\underline{n})^2 \qquad (2.1)$$

where K_{11}, K_{22} and K_{33} are the splay, twist, and bend elastic constants respectively. The total elastic energy is $U = \int dV\ F$, and there is an energy associated with the surface anchoring angle

$$\int dS\ W_o\ f(\underline{n}.\underline{k}) \qquad (2.2)$$

where W_o is the anchoring coefficient with dimensions of surface tension, $\underline{k}$ is the unit surface normal, and f is a dimensionless function with a minimum at the easy angle ψ :

$$f'(\pm\cos\psi) = 0 \qquad (2.3)$$

The sign ambiguity arises because a director $\underline{n}$ is physically equivalent[6] to $-\underline{n}$. To obtain the equilibrium director field, we minimise

$$\int dV\ (F - \tfrac{1}{2}\lambda(\underline{x})\underline{n}.\underline{n}) + \int dS\ (W_o\ f(\underline{n}.\underline{k}) - \tfrac{1}{2}\Lambda(\underline{x})\underline{n}.\underline{n}) \qquad (2.4)$$

where $\lambda(\underline{x})$ and $\Lambda(\underline{x})$ are Lagrange multipliers keeping $\underline{n}$ unit. The Euler-Lagrange equations are (with summation convention)

$$\frac{\partial F}{\partial n_i} - \frac{\partial}{\partial x_j}\left[\frac{\partial F}{\partial n_{i,j}}\right] = \lambda n_i \qquad (2.5)$$

$$k_j \frac{\partial F}{\partial n_{i,j}} + W_o\ k_i\ f'(\underline{n}.\underline{k}) = \Lambda n_i \qquad (2.6)$$

where (2.5) is true within the drop and (2.6) only on the surface of the drop. It is now clear why strong anchoring holds for large drops; the first term of (2.6) involves a space derivative of $\underline{n}$, and behaves like R^{-1} when the radius R of the drop increases, however, the second term is

independent of size scaling. From now on we shall consider only large drops. Taking (2.6) in the direction $\underline{k}$, it is dominated by the surface term :

$$W_o f'(\underline{n}.\underline{k}) + O(R^{-1}) = 0 \qquad (2.7)$$

which shows that strong anchoring prevails. The component in the direction $\underline{n}$ merely defines the field Λ, the Lagrange multiplier, or equivalently since (2.6) is the change in energy with $\underline{n}$, we can note that $\underline{n}$ is unit and cannot change along its length. The component in the remaining direction $\underline{n}\times\underline{k}$ is a zero-torque condition at the surface,

$$K_{22}\,(\underline{n}\times\underline{k})^2\,(\underline{n}.\mathrm{curl}\underline{n}) - K_{33}(\underline{n}.\underline{k})[(\underline{n}\times\underline{k}).(\underline{n}\times\mathrm{curl}\underline{n})] = 0 \qquad (2.8)$$

The surface tension W_o and anchoring energy f are now irrelevant because the drops are assumed large.

Throughout the rest of this paper we shall consider only tangential anchoring, partly because the boundary conditions simplify to

$$\underline{n}.\underline{k} = 0$$
$$\underline{n}.\mathrm{curl}\underline{n} = 0 \qquad (2.9)$$

but mainly for the reasons given in Section 1.

The energy of the drop has two parts, a surface energy proportional to R^2 and an elastic energy to proportional to R. The elastic part can be written

$$\pi R K_{11} u[\underline{n}] \qquad (2.10)$$

where u is a dimensionless functional of a director field in a unit sphere, and involves the dimensionless bend and twist elastic constants $\kappa_B = K_{33}/K_{11}$ and $\kappa_T = K_{22}/K_{11}$ respectively. The factor π has been removed for later convenience.

The energy fucntional is a sum of splay, bend and twist contributions

$$u[\underline{n}] = u_s[\underline{n}] + \kappa_B u_B[\underline{n}] + \kappa_T u_T[\underline{n}] \qquad (2.11)$$

We expect each of these three terms to contribute about equally, so that a small splay (bend, twist) constant is associated with a large u_s (u_B, u_T); in the same way as any small elastic modulus causes a large distortion.

Experimental studies indicate that tangential boundary conditions imply the bipolar configuration: there is a singularity at diametrically opposite points of the surface (the "poles"), with the director locally pointing radially away from each singularity. Under some conditions[5,7,8] the director field lines are planar, or the parity symmetry may be broken, giving a twisted appearance to the drop[2] (cf Figures 2b, 2c). We have calculated numerically[9] the director field with the one-constant approximation $\kappa_B = \kappa_T = 1$, and no other approximation, and the drop has the appearance shown in Figure 1. It can be seen that circles (overdrawn in Figure 1) which pass through both poles are a good approximation to the field lines. It is for this reason that we use an orthogonal coordinate system tailor-made for the singularities of the problem.

Bispherical coordinates (ξ,η,ϕ) consist of two poles a distance 2 apart connected by an axis of cylindrical symmetry, which is associated with the angle ϕ. Part of a plane of constant ϕ is illustrated in Figure 2a. The lines of constant η are circles passing through both poles, and the orthogonal set of constant ξ are also circles. The transformation to cylindrical coordinates (x,r,ϕ) measured from an origin midway between the poles is

$$x = Z^{-1}\cos\xi$$
$$r = Z^{-1}\sin\xi\,\sin\eta \qquad (2.12)$$

where $Z = 1 + \sin\xi\,\cos\eta$.

The quadrant in Figure 2a is the area $0 \leq \xi \leq \pi/2$, $0 \leq \eta \leq \pi/2$, and the metric elements $h_\xi = ds/d\xi$ etc, are given by

$$h_\xi = z^{-1}$$
$$h_\eta = z^{-1}\sin\xi \qquad (2.13)$$
$$h_\phi = z^{-1}\sin\xi\sin\eta$$

We now assume the director to have no $\hat{\eta}$ component, which we justify by looking at Figure 1, and write

$$\underline{n} = \hat{\xi}\cos[\tau(\eta)] + \hat{\phi}\sin[\tau(\eta)] \qquad (2.14)$$

where $\hat{\xi},\hat{\eta},\hat{\phi}$ is the triad of unit vectors, and the angle τ is the twist angle. A field line remains on a surface of constant η and ends at each of the poles, and makes a constant angle with planes through the poles. The surface $\eta = \pi/2$ is a sphere which is the surface of the drop, so the tangential anchoring condition is satisfied. Figure 2b illustrates the field lines on the surface of the drop and Figure 2c shows them on an interior surface. Using the ansatz (2.14) and the divergence theorem, after some algebra we find

$$u_s = \int dV\ \tfrac{1}{2}(\mathrm{div}\underline{n})^2 = 4\pi\int_0^{\pi/2}\frac{d\eta}{\sin^2\eta}(\eta-\cos\eta\sin\eta)\cos^2\tau \qquad (2.15a)$$

$$u_T = \int dV\ \tfrac{1}{2}(\underline{n}.\mathrm{curl}\underline{n})^2 = 2\pi\int_0^{\pi/2}d\eta\ \eta\,[d\tau/d\eta + \sin\tau\cos\tau\cot\eta]^2 \qquad (2.15b)$$

$$u_B = \int dV\ \tfrac{1}{2}(\underline{n}\times\mathrm{curl}\underline{n})^2 = \pi\int_0^{\pi/2}d\eta\ \{\frac{\eta}{\sin^2\eta}[1+\sin^2\tau+2\cos^2\eta\cos^4\tau] \qquad (2.15c)$$
$$- 3\cot\eta\cos^2\tau\}$$

It can be seen that the twist and bend energies are logarithmically infinite at the axis ($\eta\to0$) unless $\tau\to0$. If (r,z,ϕ) is a cylindrical coordinate system, the director field must be $\underline{n} = \hat{z}$ at the axis. An infinite splay energy $\underline{n} = \hat{r}$ will escape by converting to finite splay and finite bend energy[6], and an infinite bend energy $\underline{n} = \hat{\phi}$ will escape by converting to finite bend and finite twist energy[10]. Here we have the latter: indeed for small bend constant we expect the drop to have $\underline{n} = \hat{\phi}$

everywhere except near the axis, where there is a twist relaxation - this limit we call the toroidal configuration. The condition $\underline{n} = \underline{z}$, together with $\underline{n}.\mathrm{curl}\underline{n} = 0$ on the surface (cf (2.9)) give the boundary conditions for $\tau(y)$

$$\tau(0) = 0$$
$$d\tau/d\eta\big|_{\eta=\pi/2} = 0 \qquad (2.16)$$

The director configuration $\tau(\eta)$ is obtained by minimising the sum of the splay, twist and bend energies (2.15a,b,c) respectively. The Euler-Lagrange equation is

$$4\kappa_T\left(\eta\frac{d^2\tau}{d\eta^2} + \frac{d\tau}{d\eta}\right) = \sin2\tau\,[(4 - 2\kappa_T + 3\kappa_B)\cot\eta + (-4 + 2\kappa_T + \kappa_B)\,\eta\,\mathrm{cosec}^2\eta + 2\eta\cot^2\eta\,(\kappa_T - 2\kappa_B\cos^2\tau)] \qquad (2.17)$$

One solution is $\tau(\eta)=0$, corresponding to the parity-symmetric untwisted drop, with energy

$$u[\underline{n}] = u_s + \kappa_B u_B = 4 + \kappa_B(3-\pi^2/4) \qquad (2.18)$$

which has no dependence on the twist elastic constant. The ratio u_s/u_B is 7.5, so we expect this solution to be the absolute minimum when the bend constant is large.

In the rest of this Section, we make some analytic estimates of the solution $\tau(\eta)$, and in Section 3 we shall calculate it numerically.

We can calculate the energy $u[\underline{n}]$ when τ is slightly different from zero, by linearising the Euler-Lagrange equation, and solve the resulting Sturm-Liouville problem, to obtain a set of eigen functions $\tau_i(\eta)$ with eigenvalues λ_i such that for small deviations from $\tau=0$:

$$u[\textstyle\sum_i c_i\tau_i(\eta)] = \sum_i \lambda_i c_i^2 \qquad (2.19)$$

When these eigenvalues are all positive, the solution $\tau(\eta)=0$ is stable, and if the transition is second-order, the line $\min\{\lambda_i\} = 0$ in the (κ_B, κ_T) plane separates the parity-symmetric bipolar phase from the twisted phase. The lowest-λ eigenfunction will have no nodes and satisfy the boundary conditions (2.16), so we approximate it by $\sin\eta$, in which case the energy can be calculated and we find that the untwisted drop is realised when

$$\kappa_B \geq (1-\kappa_T)\,\frac{4\pi^2-16}{20-\pi^2} \simeq 2.32\,(1-\kappa_T) \qquad (2.20)$$

so that for large κ_B and for large κ_T the untwisted configuration is the minimum energy.

The only dependence on $d\tau/d\eta$ in the energy functional occurs in the twist energy. Thus when $\kappa_T=0$, the energy minimisation can be done separately at each value of η; the splay and bend energies are quadratic in $\sin^2\tau$, which can be minimised immediately,

$$\sin^2[\tau(\eta)] = \frac{1}{\kappa_B}\left(\sec^2\eta - \frac{\tan\eta}{\eta}\right) + 1 - \frac{3\tan\eta}{4\eta} - \frac{\sec^2\eta}{4} \qquad (2.21)$$

When this expression is less than zero or greater than 1, τ is 0 or $\pi/2$ respectively. When η is close to its limits,

$$\sin^2\tau \to \left(\frac{2}{3\kappa_B} - \frac{1}{2}\right)\eta^2 \qquad \eta \to 0$$

$$\sin^2\tau \to \left(\frac{1}{\kappa_B} - \frac{1}{4}\right)(\pi/2-\eta)^{-2} \qquad \eta \to \pi/2 \qquad (2.22)$$

For $\kappa_B > 4$ the untwisted bipolar drop is preferred; for $\kappa_B > 4/3$ there is part untwisted (small η) and part with $\tau=\pi/2$; and for $\kappa_B < 4/3$, there is twist for all $\eta > 0$, with $\tau=\pi/2$ for the larger values.

We shall now investigate the response of the drop to a weak magnetic field. The nematogen molecules tend to line up parallel to the field, so we expect the untwisted drop to have its axis parallel, and the limiting toroidal drop to have its axis normal to the field. If the field is not

weak, the director field will be distorted, and in the toroidal case lose axial symmetry, so that all the analysis of this paper would be invalid. We would, however, expect a second-order phase transition to be associated with the loss of axial symmetry, and we shall calculate the transition line in the weak field case.

The energy density associated with the magnetic field is proportional[6] to $(\underline{n}.\underline{B})^2$, and for axisymmetric drops, we find that the axis is parallel to the field if

$$1/3 \leq V^{-1} \int dV\, (\underline{n}.\hat{\underline{x}})^2 \qquad (2.23)$$

$$= 3\int_0^{\pi/2} d\xi \int_0^{\pi/2} d\eta h_\xi h_\eta h_\phi \frac{(\sin\xi + \cos\eta)^2}{Z^4}\cos^2\tau(\eta)$$

where Z is from (2.12) and $h_\xi h_\eta h_\phi$ is the volume element from (2.13). This quantity is the average of the square of the component of $\underline{n}$ along the axis: for the untwisted drop with $\tau=0$ it is 79/150, so the axis is parallel to the field, as observed experimentally[5]. For the toroidal drop $\tau=\pi/2$ and the average is zero, so the drop axis is normal, as surmised above.

3. Calculation

The Euler-Lagrange equation (2.17) is of boundary-layer type near $\eta=0$, which is caused by the small quantity η multiplying the highest derivative. We can remove this singularity by transforming to the independent variable $y=\ln(2\eta/\pi)$ so that

$$\frac{d^2\tau}{dy^2} = \eta^2 \frac{d^2\tau}{d\eta^2} + \eta \frac{d\tau}{d\eta} \qquad (3.1)$$

The boundary conditions for $\tau(\eta)$ are now

$$\frac{d\tau}{dy}(y=0) = 0 \qquad (3.2a)$$

$$\tau\,(y \to -\infty) = 0 \qquad (3.2b)$$

We directly minimise the energy $u[\underline{n}]$ by the method of successive over-relaxation[11]. First we choose a large negative number y_{min} and discretise the interval $(y_{min},0)$ with spacing h. The energy is then quadratic in the discretised values τ_i, and we cycle through these points adjusting τ_i to minimise the energy locally. This process is completely equivalent to the numerical solution of the diffusion-like equation of Euler-Lagrange form:

$$\frac{\partial\tau}{\partial t} = -\frac{\partial F}{\partial \tau} + \frac{\partial}{\partial y}\left[\frac{\partial F}{\partial \tau'}\right] \qquad (3.3)$$

We find that the energy decreases monotonically to a limit, and we used the convergence criterion that the change in each τ_i per step should be less than 10^{-4} radians. We then make y_{min} more negative and repeat the relaxation. This is continued until a further decrease in y_{min} makes no difference within the above criterion.

The resulting solution $\tau(\eta)$ can be characterised by the elastic energy $u[\underline{n}]$, the exterior twist angle $\tau(\eta=\pi/2)$, and the initial slope $d\tau/d\eta$ $(\eta=0)$: these are shown in Figures 3, 4 and 5 respectively as contour plots in the (κ_B,κ_T) plane.

In each of these Figures, the most obvious feature is the curved line joining $\kappa_T=1$, $\kappa_B=0$ to $\kappa_T=0$, $\kappa_B=4$, which is the second-order parity-breaking phase transition from untwisted to twisted droplets. When κ_T is large, the condition (2.20) is a good approximation: the dashed line in the figures is the continuation of that straight line. When κ_T is zero, the analysis (2.22) indicates that $\kappa_B=4$ is a transition point: this is marked in the figures. The planar part of the energy surface in Figure 3 is the exact expression (2.18), and the energy is zero at $\kappa_B=0$, $\kappa_T=0$, because this is the limiting toroidal case $\tau=\pi/2$ which has no splay energy.

In Figure 5 is the slope of $\tau(\eta)$ at $\eta=0$. When this is large the twist angle rises sharply to $\pi/2$ and stays there, so the director is azimuthal except near the axis, where there is a disclination. The width of this disclination is proportional to $\sqrt{\kappa_B}$ when κ_B is small. The surface twist angle in Figure 4 is $\pi/2$ for small κ_B or small κ_T, and has a square-root singularity at the phase-transition line.

We have calculated the double integral (2.23) by Simpsons rule with 50 points each way, and the chained line in Figure 5 shows where it is 1/3, and is the transition from the drop axis being parallel to normal (to a weak magnetic field).

Also marked on Figure 4 are some experimental measurements of nematics[12]. All except one of these are short-rod nematics, and one (PBG, poly-γ-benzyl-glutamate) is a polymer. These may not be tangentially anchored, although it is known that temperature[3], concentration, and surfactant[8] can all change the anchoring angle. It is clear, however, that short-rod nematics generally lie outside the twisted region, although APAPA9 should be somewhat twisted. The measurement of the elastic constants of PBG is recent, and bears out theoretical studies[10,13] of elastic constants of nematic polymers. We predict that if an interface prefers tangential anchoring, then PBG should exhibit highly twisted droplets.

4. Conclusions

We have taken a simple approximation to the elastic energy functional for a nematic droplet, and shown that a phase transition to a twisted configuration occurs for large splay constant. While we do not expect our results to be quantitatively correct, in view of the approximation, it is reasonable to expect the main features to be qualitatively accurate. A treatment using the full elastic energy functional could be used to measure elastic constants, especially since some nematics will be just inside the twisted region, giving great sensitivity.

In a magnetic field, the director tends to align parallel to the field. For the untwisted drop, the axis must then be parallel, but for sufficiently large splay constant, the axis is perpendicular. In this case the drop will cease to be axisymmetric, so we expect a second-order phase transition. As above, any finite magnetic field will distort the drop and move the transition line, but the qualitative conclusion does not change.

Although elastic constants are available for only one polymer nematic, theoretical work suggests that the relatively small K_{22} and K_{33} are generic features, so it would be interesting to observe droplets of polymer nematic to measure their twist characteristics, perhaps by polarised light scattering. The concentration of polymer affects the elastic constants, and these twisted drops would be a good way of observing such variation.

References

[1] S Faetti and V Palleschi, Phys Rev A30 (1984) 3241

[2] M J Press and A S Arrott, Phys Rev Lett 33 (1974) 403; J Physique 36 (1975) C1-177

[3] G E Volovik and O D Lavrentovich, Zh Eksp Teor Fiz 85 (1983) 1997 [JETP 58 (1984) 1159]; M J Kurik and O D Lavrentovich, Pis'ma Zh Eksp Teor Fiz 35 (1982) 362 [JETP Lett 35 (1982) 444]

[4] S Chandrasekhar, "Liquid Crystal Conference, Kent, Ohio 1965" (Gordon and Breach, New York)

[5] E Dubois-Violette and O Parodi, J Physique C4 30 (1969) 57

[6] P G de Gennes "The Physics of Liquid Crystals", (Oxford UP, 1974)

[7] N V Madhusudana and K R Sumathy, Mol Cryst Liq Cryst Lett 92 (1983) 179

[8] S Candau, P le Roy and F Debeauvais, Mol Cryst Liq Cryst 23 (1973) 283

[9] R D Williams, Rutherford Appleton Laboratory Report RAL-85-028

[10] R B Meyer in "Polymer Liquid Crystals" eds A Ciferri, W R Krigbaum and R B Meyer (Academic Press 1982), Chapter 6

[11] W E Milne "Numerical Solution of Differential Equations", (Dover, New York, 1970)

[12] Elastic Constants,
PBG: V G Taratuta, A J Hurd and R B Meyer, Phys Rev Lett 55 (1985) 246
MBBA: E Miraldi, L Trossi and P Taverna Valabrega, Nuovo Cim 66B (1981) 179

MBCA, APAPA: F Leenhouts, A J Dekker and W H de Jeu, Phys Lett 72A (1979) 155

PAA: H Gruler, Z Naturforsch 28A (1973) 474

OHMBBA, APAPA9: F Leenhouts and A J Dekker, J Chem Phys 74 (1981) 1956

[13] P G de Gennes, Chapter 5 of Ref 10

Figure Captions

Figure 1 Exact director configuration in the one-constant approximation, from Ref 9, with overlaid circles to show goodness of fit.

Figure 2 (a) Bispherical coordinate system with unit vectors. The vector $\underline{\phi}$ is normal to the paper.

(b) Director field lines for $\tau(\pi/2)=29°$.

(c) Field lines for $\eta=25°$, $\tau(\eta)=22°$.

Figure 3 Dimensionless energy $u[\underline{n}]$ as a contour plot in the plane $\kappa_B=K_{33}/K_{11}$, $\kappa_T=K_{22}/K_{11}$. The contour spacing is 0.5. The thin line is the phase transition line.

Figure 4 Contour plot of the surface twist angle $\tau(\eta)$ at $\eta=\pi/2$, with contour interval 10°. Data for some short-rod nematics is from Reference 12; the dashed line for PAP is a temperature variation, and the disk for MBBA is an error estimate.

Figure 5 Contour plot of the internal twist $d\tau/d\eta$ at $\eta=0$, which is the twist disclination strength at the axis.

1

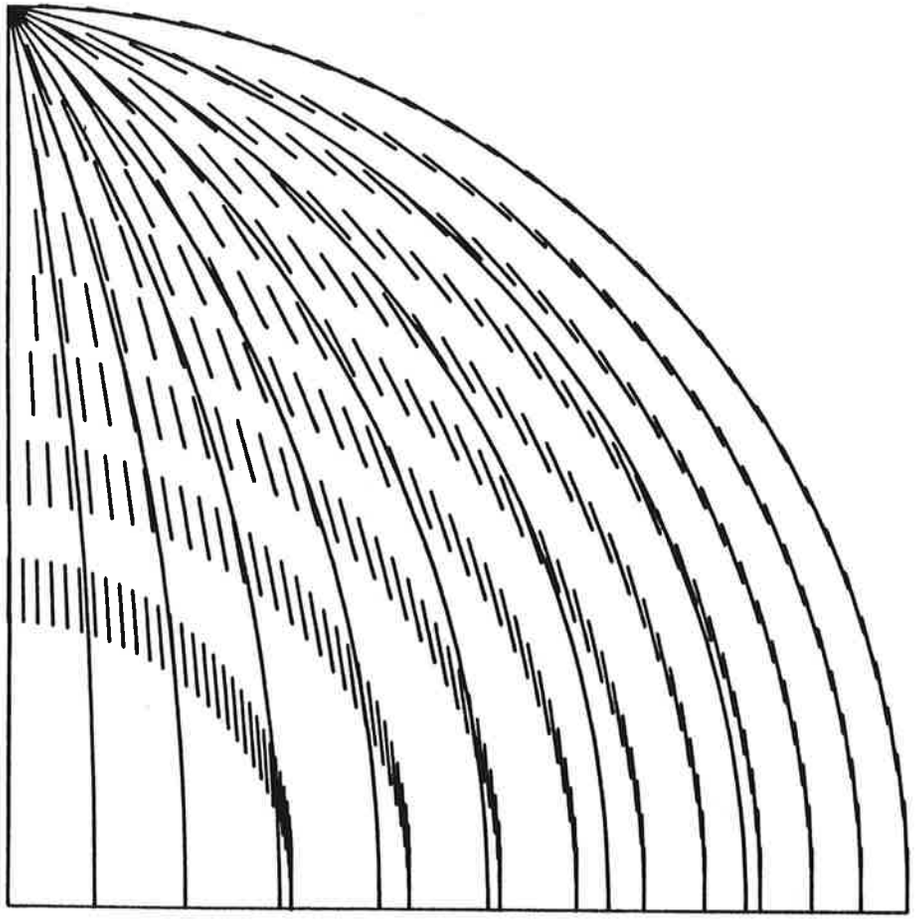

2 (a)

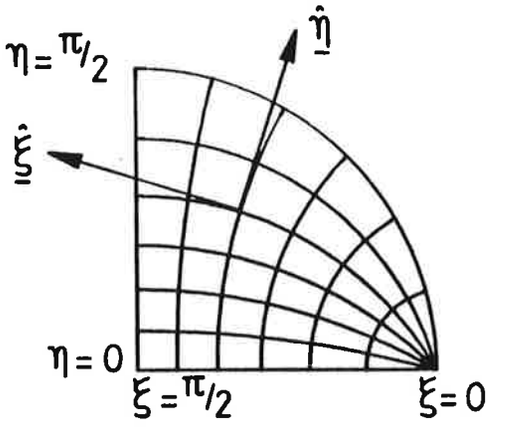

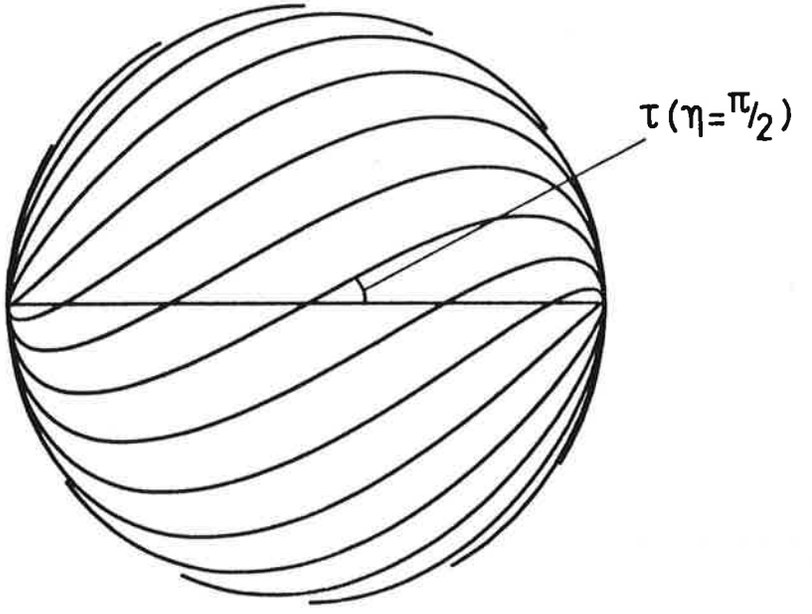

2 (b)

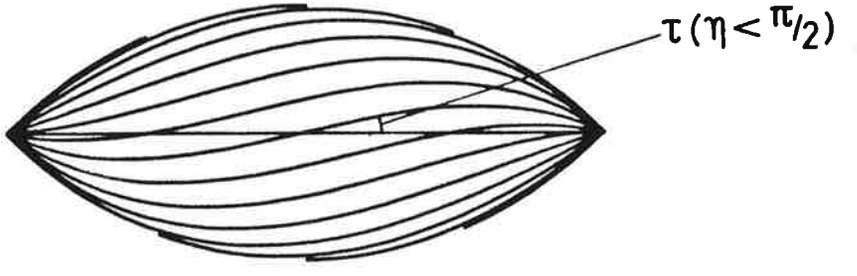

2 (c)

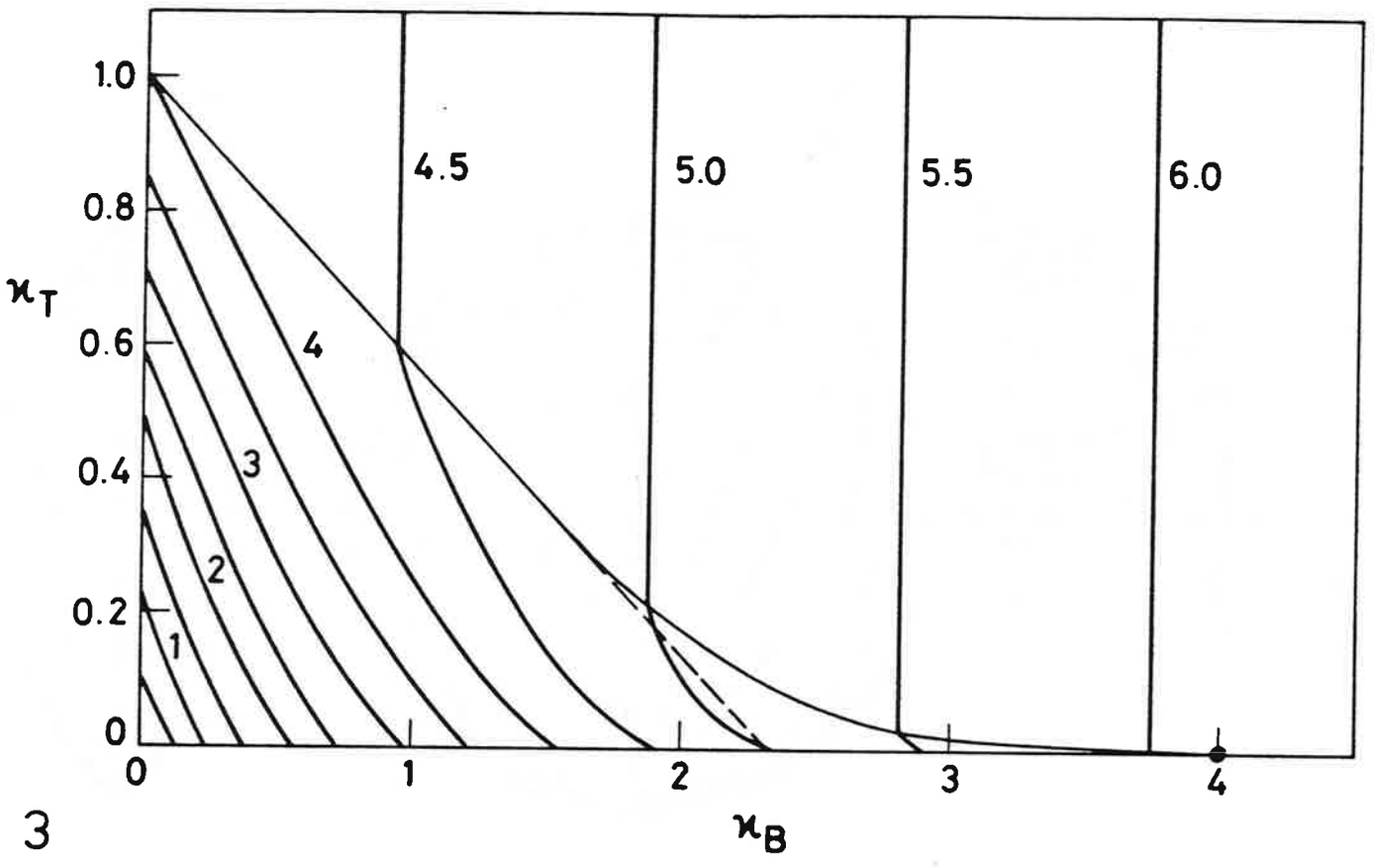
1.0
0.8
0.6
0.4
0.2
0
$\varkappa_T$
4.5
5.0
5.5
6.0
4
3
2
1
0
1
2
3
4
$\varkappa_B$

3

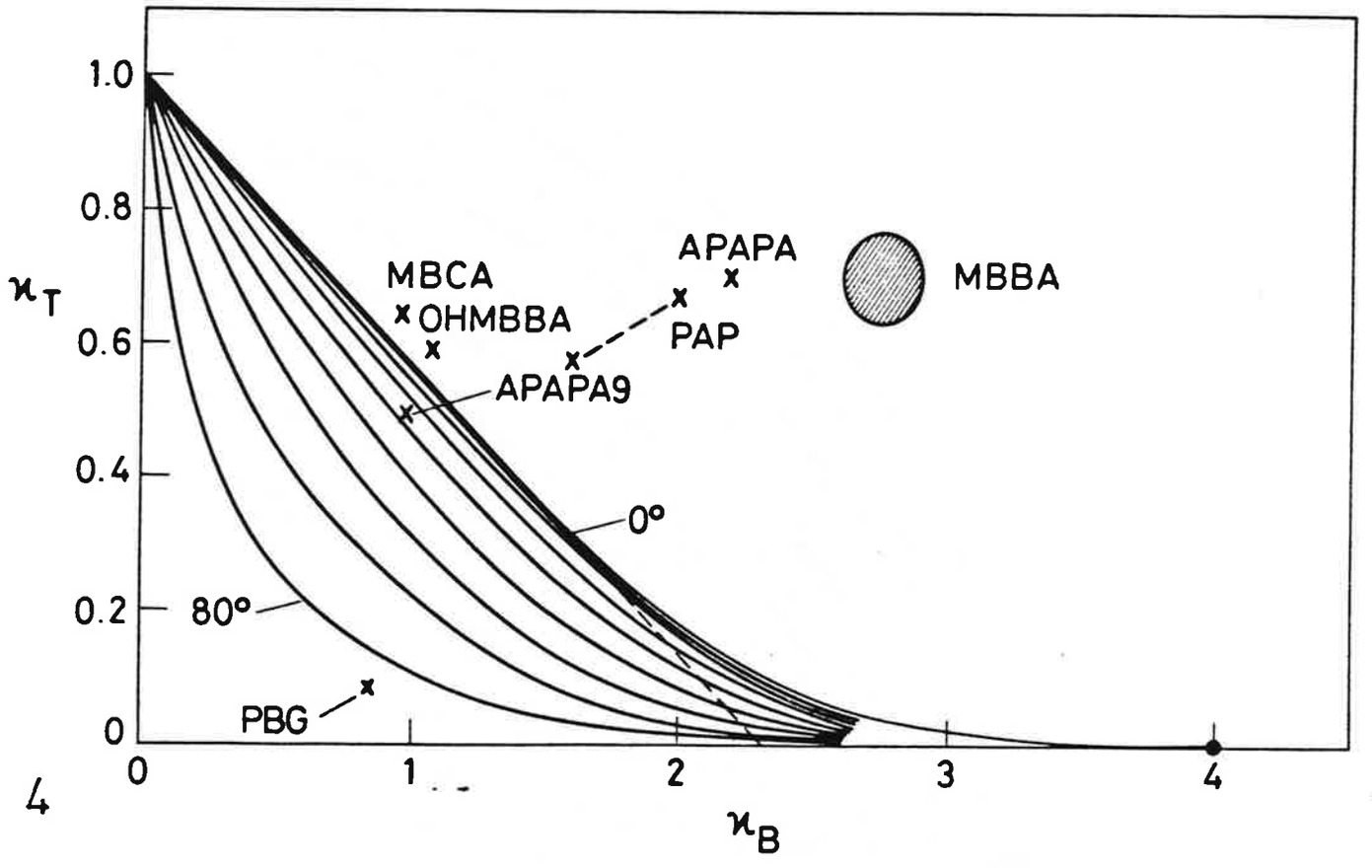
1.0
0.8
0.6
0.4
0.2
0
$\varkappa_T$
MBCA
OHMBBA
APAPA
PAP
APAPA9
MBBA
0°
80°
PBG
0
1
2
3
4
$\varkappa_B$

4

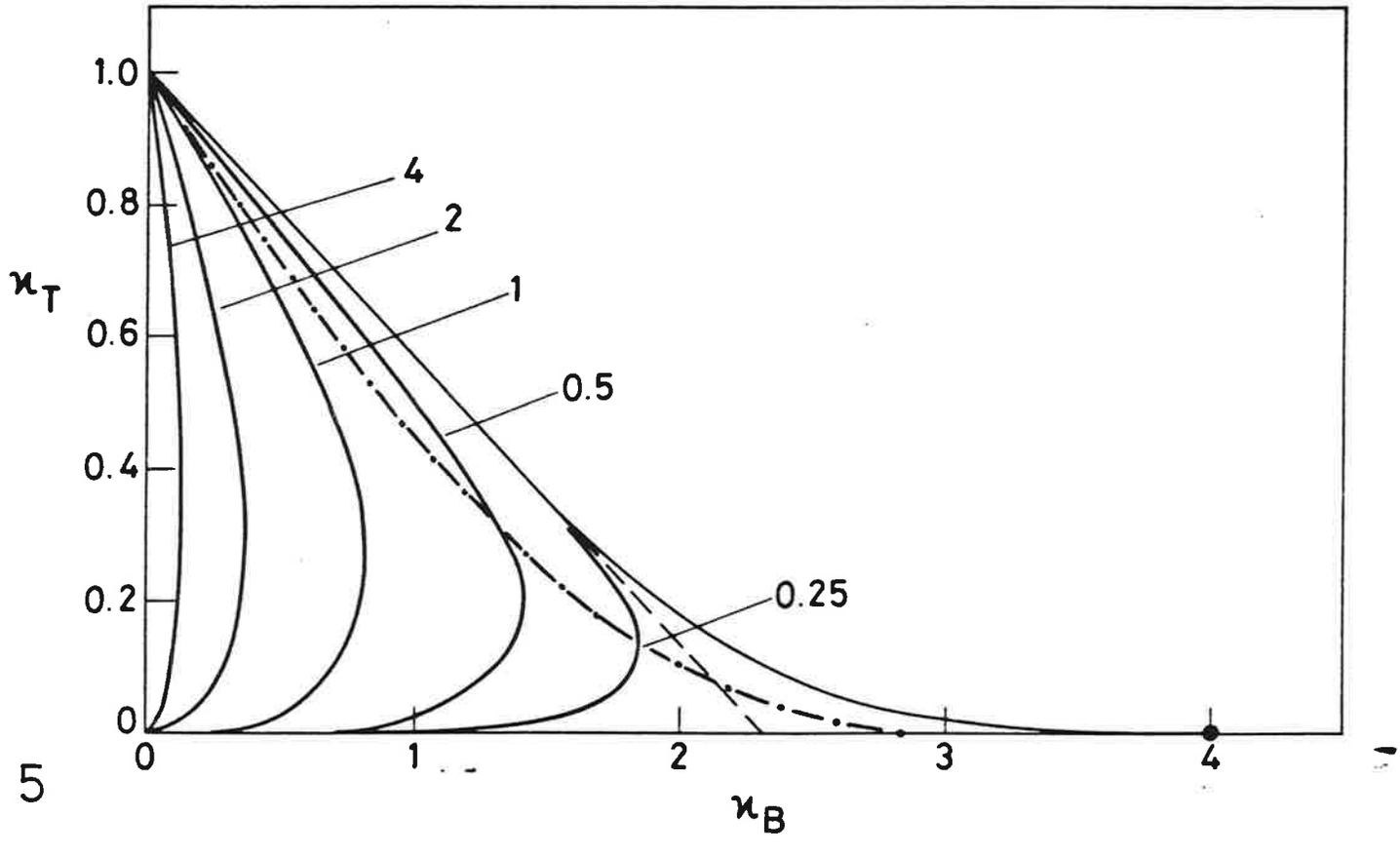

5